Coherent control of tunneling in driven tight-binding chains: Perturbative analysis

Stefano Longhi

Dipartimento di Fisica and Istituto di Fotonica e Nanotecnologie del CNR, Politecnico di Milano, Piazza L. da Vinci 32, I-20133 Milan, Italy

(Received 6 February 2008; revised manuscript received 21 April 2008; published 28 May 2008)

Coherent control of quantum tunneling in an ac-driven tight-binding chain made of a finite number of positional sites, such as electronic tunneling in finite superlattices of quantum wells or in linear chains of quantum dots driven by a sinusoidal electric field, is analytically investigated in the large-frequency regime by a multiple-scale asymptotic analysis of the underlying equations, which is exact up to the normalized time scale $\sim 1/\epsilon^3$, where $\epsilon=\Delta/\omega$ is the ratio between the hopping amplitude Δ of adjacent sites and the modulation frequency ω. The results of the analysis are applied to tunneling control in linear chains with $N=2$, 3, 4, 5, and 6 potential wells. For a double-well system ($N=2$), the usual condition for coherent destruction of tunneling (CDT) of a driven two-level system, with a third-order correction term, is retrieved. For an array comprising $N=3$, 5, or 6 sites, crossing and anticrossing in the quasienergy spectrum near a collapse point, which result in selective CDT, are found according to the numerical (nonperturbative) results previously presented by Villas-Bôas *et al.* for driven quantum-dot arrays [Phys. Rev. B **70**, 041302 (2003)]. The behavior of quasienergy crossings and avoided crossings for the multiple-well array found in the framework of the third-order perturbative theory is shown to be consistent with the predictions based on generalized symmetries of the Floquet states.

DOI: 10.1103/PhysRevB.77.195326 PACS number(s): 73.23.−b, 73.40.Gk, 78.67.Hc, 72.20.Ht

I. INTRODUCTION

Coherent control of tunneling and electronic transport in semiconductor superlattices and arrays of coupled quantum dots or quantum wires has received in recent years a considerable and increasing interest from both theoretical and experimental sides (see, for instance, Refs. 1–5 and references therein). Preservation of the quantum coherence of the electronic states can give rise to unusual transport phenomena when an ac electric field is applied to the system, with the most notable ones being the coherent destruction of tunneling[4,6] (CDT) and dynamic localization[3–5,7] (DL). DL refers to the phenomenon that a localized electron in a tight-binding lattice driven by an external ac electric field periodically returns to its initial state following the periodic change in the field, thereby suppressing quantum diffusion in the lattice. Such an effect has been extensively investigated for semiconductor superlattices[3,8–11] and was related to the collapse of quasienergy minibands.[8] CDT refers to suppression of tunneling of a particle between the two wells of an ac-driven bistable potential and, in its simplest model, it is related to the problem of level crossing in driven two-level systems.[4,12–16] In both CDT and DL, the degree of suppression and localization sensitively depends on the parameters of the driving field, thereby giving the attractive possibility of coherently manipulating electronic states in arrays of coupled quantum wells or quantum dots by means of laser pulses or oscillating gate potentials (see, for instance, Refs. 17–20). For, e.g., a sinusoidal electric field $E(t)=\mathcal{E}_0\cos(\omega t)$, in the large-frequency limit—where the ac field frequency ω is sufficiently larger than the hopping rate Δ between adjacent wells— the condition for CDT is given by the approximate relation $J_0(e\mathcal{E}_0 d/\hbar\omega)=0$, where d is the separation between adjacent wells. Even in the large-frequency limit, CDT in a tight-binding chain with a *finite* number $N\geq 4$ of coupled wells, however, is usually an *approximate* effect that holds when considering the system dynamics up to a time scale of the order $\sim 1/\epsilon$, as compared to the modulation cycle, where $\epsilon=\Delta/\omega$. This is due to the fact that the quasienergies for the finite chain do not show an exact crossing when the field amplitude $\mathcal{E}_0$ is varied, rather a fine structure of crossings and avoided crossings is observed in numerical simulations near the $J_0(e\mathcal{E}_0 d/\hbar\omega)=0$ collapse points. In particular, Holthaus and Hone[8] numerically showed that lattice truncation is responsible for a pseudocollapse of quasienergy minibands in semiconductor superlattices, and thus DL is imperfect in finite structures. This was also shown by Raghavan *et al.*[21] in numerical simulations of particle tunneling in a finite chain of coupled wells within the nearest-neighbor tight-binding (NNTB) approximation. In the framework of the same tight-binding model, in a recent work, Villas-Bôas *et al.*[18] numerically studied the tunneling dynamics of ac-driven quantum-dot arrays made of a relatively small number of dots, showing the existence of a complex and size-dependent crossing and avoided crossing scenario in the quasienergies near the collapse point. It was also proposed that the fine structure of quasienergies near the pseudocrossing point can be conveniently exploited for selective CDT among different dots in the array.[18] In these previous studies, even within the NNTB approximation, the problem was treated by full numerical simulations, and an approximate model to capture the main dynamical features is missing. Unfortunately, a simple first-order perturbative analysis in the large-frequency limit, similar to the one previously adopted for driven two-level systems (see, for instance, Refs. 12, 13, and 16), fails to capture the fine structure of the quasienergy spectrum which is needed to explain, for instance, the selective CDT scenario numerically found in Ref. 18 A more refined perturbative theory to describe tunneling control in a tight-binding chain driven by a bichromatic field, which is accurate up to the time scale $\sim 1/\epsilon^2$, was presented

in Ref. 17, however, it is not accurate in case of a monochromatic driving field.

In this work, we present a perturbative analysis of tunneling control in ac-driven linear chains of coupled quantum wells or quantum dots in the large-frequency limit based on a multiple-scale asymptotic expansion of the underling equations describing tunneling dynamics in the NNTB approximation. The perturbative analysis is applied, as an example, to tunneling control by sinusoidal driving in chains made of $N=2,3,4,5$, and 6 sites. For the simplest case of a double-well system ($N=2$), our theory yields a third-order correction term to the leading-order Floquet quasienergies, according to previous strong-coupling theories of sinusoidally driven two-level systems.[15,22] For the triple-well system ($N=3$), we show that CDT is still an exact result. For $N=4$, 5, or 6 wells, our analytical results are accurate enough to reproduce crossings and avoided crossings of quasienergies near the collapse point in agreement with general grounds based on the generalized symmetries of Floquet states. In addition, the perturbative analysis provides a simple and analytical explanation of selective CDT in quantum-dot arrays proposed in Ref. 18

The paper is organized as follows. In Sec. II, the basic model of an ac-driven tight-binding chain is presented, and a first-order analysis of quasienergies in the large-frequency limit is shown to be inaccurate to describe tunneling dynamics in the chain. In Sec. III, a multiple-scale asymptotic analysis of the underlying equations is performed, and the asymptotic evolution of the system up to the time scale $\sim 1/\epsilon^3$ is derived. Section IV specializes the general results of Sec. III to coherent tunneling control in a chain made of $N=2$, 3, 4, 5, or 6 wells. The behavior of quasienergy crossings and anticrossings near a collapse point predicted by the perturbative analysis is shown to be consistent with the results based on dynamical symmetries of the Floquet states and capable of explaining in a simple way the selective CDT numerically studied in Ref. 18.

II. TUNNELING IN AC-DRIVEN TIGHT-BINDING CHAINS: BASIC MODEL AND FIRST-ORDER PERTURBATION THEORY

A. Model

The starting point of our analysis is provided by a rather standard model describing electron tunneling in a chain of potential wells, separated each other by the same distance d and driven by a strong ac electric field $E(t)$ of frequency ω, which provides a simplified model previously used to describe coherent tunneling control in semiconductor superlattices or in arrays of quantum dots (see, for instance, Refs. 17, 18, 21, 23, and 24). We assume that the localized states $|n\rangle$ at various sites in the chain have (approximately) the same energy in the absence of the external field and indicate by Δ_n the hopping rate between adjacent sites $|n\rangle$ and $|n+1\rangle$ (see Fig. 1).

In the NNTB approximation, for a single electron, the appropriate Hamiltonian is given by (see, for instance, Ref. 17)

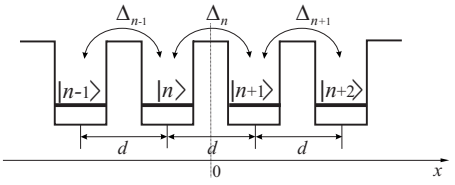

FIG. 1. Schematic of quantum tunneling in a chain of coupled quantum wells.

$$H = \hbar \sum_n \Delta_n (|n\rangle\langle n+1| + |n+1\rangle\langle n|) + + edE(t) \sum_n n|n\rangle\langle n|, \tag{1}$$

where $|n\rangle$ is the localized state at the site n. Note that the case of a finite chain made of N equal wells with the same hopping amplitudes Δ is simply obtained from the previous Hamiltonian after setting $\Delta_n=\Delta$ for $1\leq n\leq N-1$ and $\Delta_n=0$ otherwise. By expanding the electronic quantum state $|\psi(t)\rangle$ as a superposition of localized states $|n\rangle$, $|\psi(t)\rangle=\Sigma_n c_n(t)|n\rangle$, the coupled mode equations for the amplitudes c_n derived from Hamiltonian (1) explicitly read

$$i\dot{c}_n = (\Delta_n c_{n+1} + \Delta_{n-1} c_{n-1}) + \frac{edE(t)}{\hbar} n c_n, \tag{2}$$

where the dot indicates the derivative with respect to time. For the following analysis, it is worth introducing, in place of c_n, the amplitudes a_n defined by the relations

$$c_n(t) = a_n(t) \exp\left[-in\frac{ed}{\hbar} \int_0^t dt' E(t') - in\rho \right], \tag{3}$$

so that Eq. (2) takes the form

$$i\dot{a}_n = \Delta_n F(t) a_{n+1} + \Delta_{n-1} F^*(t) a_{n-1}, \tag{4}$$

where we have set

$$F(t) = \exp\left[-i\frac{ed}{\hbar} \int_0^t dt' E(t') - i\rho \right], \tag{5}$$

$\rho \equiv -[ed/(2\hbar)]\int_0^{T/2} dt E(t)$, and $T=2\pi/\omega$ is the period of the ac electric field. Note that $F(t)$ can be expanded in the Fourier series according to

$$F(t) = F_0 + \sum_{l\neq 0} F_l \exp(-il\omega t), \tag{6}$$

where F_0 is the cycle-average value (i.e., the dc value) of $F(t)$. Note also that, as the dc value of the electric field $E(t)$ is zero, in general, F_0 does not vanish. For the special case of a sinusoidal ac field,

$$E(t) = \mathcal{E}_0 \cos(\omega t + \varphi), \tag{7}$$

one obtains

$$F_l = J_l\left(\frac{ed\mathcal{E}_0}{\hbar\omega} \right) \exp(-il\varphi). \tag{8}$$

Owing to the periodicity of $F(t)$, the most general solution to Eq. (4) is given by an arbitrary linear superposition of the Floquet states $a_n(t)=u_n^{(l)}(t)\exp(-i\mu_l t)$, where $u_n^{(l)}(t+2\pi/\omega)$

$=u_n^{(l)}(t)$ is the periodic part of the Floquet state and $E_l \equiv \hbar\mu_l$ is the corresponding quasienergy, which is uniquely defined inside the first "Brillouin zone" $-\hbar\omega/2 \le E_l < \hbar\omega/2$. Note that, for a finite chain of size N, there are N quasienergies, i.e., $l=1,2,\ldots,N$. The tunneling dynamics of the electron in the chain is strongly determined by the relative values of quasienergies, which can be controlled by varying frequency and amplitude of the ac electric field. In particular, the phenomenon of CDT corresponds to a *simultaneous* exact crossing of quasienergies E_l and to a modulation frequency ω large enough in such a way that, over one modulation cycle, the periodic parts $u_n^{(l)}$ of the Floquet states show small oscillations. The latter condition is typically satisfied for a modulation frequency ω sufficiently larger than the hopping rates Δ_n, whereas the former condition is usually not met in a *finite* chain made of $N \ge 4$ sites, where a complex pattern of level crossings and avoided crossings is observed (see, for instance, Ref. 18). In most common situations, invariance of the underlying Hamiltonian for simultaneous time translation $t \to t+T/2$ and spatial reflection $x \to -x$ results in special generalized symmetries of the Floquet states, which largely influence the pattern of quasienergy crossings and avoided crossings for a multiple-well system. This point will be discussed in details in Sec. IV A and in Appendixes A and B for a specific model.

B. Large-frequency limit: First-order perturbation theory

The large-frequency limit is attained when the modulation frequency ω is sufficiently larger than the hopping rates Δ_n between adjacent sites in the chain. In this case, it is worth rescaling the time variable t to the modulation cycle by the change $t'=\omega t$ and setting $\mathbf{a}=(\cdots,a_{n-1},a_n,a_{n+1},\cdots)^T$, $\Delta_n \equiv \epsilon\omega\theta_n$, where $\epsilon \ll 1$ and $\theta_n \sim 1$. Equations (4) can be then cast into the compact matrix form suited for a perturbative analysis,

$$i\dot{\mathbf{a}} = \epsilon\mathcal{M}(t')\mathbf{a}, \tag{9}$$

where the matrix $\mathcal{M}(t')$ is periodic in the time t' with period 2π $[\mathcal{M}(t'+2\pi)=\mathcal{M}(t')]$. The elements of the matrix $\mathcal{M}$ are explicitly given by

$$\mathcal{M}_{n,m} = \theta_n F(t')\delta_{n,m-1} + \theta_{n-1}F^*(t')\delta_{n,m+1}, \tag{10}$$

where

$$F(t') = F_0 + \sum_{l\neq 0} F_l \exp(-ilt'). \tag{11}$$

Equation (9) indicates that the change in amplitude $\mathbf{a}$ over one modulation cycle is small (of order $\sim\epsilon$), and therefore at first approximation, the temporal evolution of $\mathbf{a}$ is dominated by the cycle-average terms of $\mathcal{M}(t')$, i.e., one can write at leading order

$$i\dot{\mathbf{a}} \simeq \epsilon\overline{\mathcal{M}(t')}\mathbf{a}, \tag{12}$$

where the overline denotes the time-average over the modulation cycle, i.e.,

$$\overline{\mathcal{M}(t')}_{n,m} = \theta_n F_0 \delta_{n,m-1} + \theta_{n-1}F_0^*\delta_{n,m+1}. \tag{13}$$

This is the well-known rotating-wave (or averaging) approximation commonly used to study CDT in the large-frequency limit for the driven double-well problem (see, for instance, Refs. 12 and 13). In this case, the quasienergies E_l are simply given by $E_l=\hbar\omega\epsilon\lambda_l$, where λ_l are the eigenvalues of the cycle-averaged matrix $\bar{\mathcal{M}}$. The rotating-wave approximation provides an accurate description of quasienergy spectrum and of temporal evolution of amplitudes a_n provided that $F_0 \sim O(1)$. If F_0 vanishes or gets small (of order $\sim\epsilon$ or smaller), the rotating-wave approximation [Eq. (12)] indicates that the amplitudes a_n do not vary with time over the time scale $1/\epsilon$ and, correspondingly, there is a collapse of quasienergies. However, such a result is only approximated because the amplitudes a_n may vary on a time scale *longer* than $\sim 1/\epsilon$ and, correspondingly, the collapse of quasienergies is actually a *pseudocollapse*. To better explain this point, let us consider the case of a sinusoidal electric field [Eq. (7)]. For a double-well system, the condition $F_0=0$ corresponds to $J_0(ed\mathcal{E}_0/\hbar\omega)=0$ [see Eq. (8)], which is the well-known condition for CDT in the large-frequency limit as obtained by the rotating-wave approximation.[12,13] If we consider the first zero of Bessel function, the electric field amplitude $\mathcal{E}_0$ for CDT is thus given by $\mathcal{E}_0 \simeq 2.405\hbar\omega/(ed)$. More refined perturbative analyses for the driven two-level system show that a third-order correction term should be included in the expression of quasienergies (see, for instance, Refs. 15 and 22). However, such a correction is merely responsible for a small *shift* of the field amplitude $\mathcal{E}_0$ at which exact crossing of quasienergies (and thus CDT) occurs. Conversely, for multiple-well chains, such as those considered in Ref. 18, accurate numerical simulations show that, near the collapse region $\mathcal{E}_0 \simeq 2.405\hbar\omega/(ed)$, there is a more complex and size-dependent crossing and anticrossing scenario of quasienergies (see, for instance, Figs. 1 and 5 of Ref. 18), which is fully missed in first-order perturbation theory [Eq. (12)] but which is crucial to achieve a selective CDT as proposed in Ref. 18. A more accurate perturbative analysis, which is capable of capturing the behavior of quasienergies near the collapse point and consistent with general results based on the dynamical symmetries of the Floquet states (as discussed in details in Sec. IV), is therefore needed in order to correctly study tunneling dynamics and control in a multiple-well array.

III. MULTIPLE-SCALE ASYMPTOTIC ANALYSIS

The main reason for the failure of the averaging method to capture the behavior of quasienergies near the collapse point for a multiple-well array, as discussed in Sec. II B, is due to the fact that, as the averaging technique provides a correct description of the temporal evolution of amplitudes a_n up to the time scale $\sim 1/\epsilon$, the detailed behavior of quasienergies near the collapse point is related to the temporal dynamics at longer time scales $\sim 1/\epsilon^2$, $\sim 1/\epsilon^3,\cdots$. It is therefore mandatory to include in the perturbative analysis the system evolution at longer time scales, which can be done by a multiple-scale asymptotic analysis of Eq. (9). To

this aim, we seek for a solution to Eq. (9) as a power series in the smallness parameter ϵ,

$$\mathbf{a} = \mathbf{a}^{(0)} + \epsilon \mathbf{a}^{(1)} + \epsilon^2 \mathbf{a}^{(2)} + \cdots, \tag{14}$$

and introduce multiple scales for time, i.e., we assume that the amplitude $\mathbf{a}$ depends on $T_0, T_1, T_2, T_3, \ldots$, where

$$T_0 = t', T_1 = \epsilon t', T_2 = \epsilon^2 t', T_3 = \epsilon^3 t', \cdots, \tag{15}$$

As the quasienergy collapse point is attained when $\overline{\mathcal{M}(t')} = 0$, for the following analysis, it is useful to write

$$\mathcal{M}(T_0) = \mathcal{A} + \mathcal{B}(T_0), \tag{16}$$

where $\mathcal{A} \equiv \overline{\mathcal{M}(t')}$ is the dc term of $\mathcal{M}(t')$, whereas $\mathcal{B}(T_0)$ is the ac part of $\mathcal{M}(t')$, i.e., see Eqs. (10) and (11),

$$\mathcal{A}_{n,m} = \theta_n F_0 \delta_{n,m-1} + \theta_{n-1} F_0^* \delta_{n,m+1}, \tag{17}$$

$$\mathcal{B}_{n,m}(T_0) = \theta_n \left[\sum_{l \neq 0} F_l \exp(-ilT_0) \right] \delta_{n,m-1} + \theta_{n-1} \left[\sum_{l \neq 0} F_l^* \exp(ilT_0) \right] \delta_{n,m+1}. \tag{18}$$

For a given modulation frequency, the order of magnitude of $\mathcal{A}$ is typically controlled by the electric field amplitude and may get small (of order $\sim\epsilon$ or smaller) or even vanish for certain values of the field amplitude, as discussed in Sec. II B. Conversely, $\mathcal{B}$ is expected to be of order ~ 1 independently of the electric field amplitude because it is likely that there will be at least one Fourier coefficient F_l which is finite. It is then useful to write $F_0 = F_0^{(0)} + \epsilon F_0^{(1)} + \epsilon^2 F_0^{(2)} + \cdots$ and, correspondingly, we get for $\mathcal{A}$ the expansion

$$\mathcal{A} = \mathcal{A}^{(0)} + \epsilon \mathcal{A}^{(1)} + \epsilon^2 \mathcal{A}^{(2)} + \cdots. \tag{19}$$

In the above expansion, it is intended that there is solely one nonvanishing term that defines the order of magnitude of F_0 and hence of $\mathcal{A}$. For instance, for a sinusoidal modulation, the order of magnitude of F_0 is that of $J_0(ed\mathcal{E}_0/\hbar\omega)$, and therefore for an electric field amplitude $\mathcal{E}_0$ close to the quasienergy collapse point, one should take $\mathcal{A} \sim \epsilon^l$ for some integer $l \geq 1$, and hence $\mathcal{A}^{(k)} = 0$ for $k \neq l$. Far from the collapse point and for $J_0(ed\mathcal{E}_0/\hbar\omega) \sim 1$, one instead will assume $\mathcal{A}^{(k)} = 0$ for $k \geq 1$.

Substituting *Ansätze* (14), (16), and (19) into Eq. (9), using the derivative rule $d/dt' = \partial_{T_0} + \epsilon \partial_{T_1} + \epsilon^2 \partial_{T_2} + \epsilon^3 \partial_{T_3} + \cdots$ and collecting the terms of the same order in the equation to obtained, a hierarchy of equations for successive corrections to $\mathbf{a}$ is obtained. At leading order ($\sim\epsilon^0$), one obtains

$$\mathbf{a}^{(0)} = \mathbf{A}(T_1, T_2, T_3, \cdots), \tag{20}$$

where $\mathbf{A}$ is an arbitrary vectorial function of slow time variables $T_1, T_2, T_3, \cdots$, but it is constant with respect to T_0, i.e., $\partial_{T_0}\mathbf{A} = 0$. The equations at higher orders $\sim\epsilon^k$ (with $k \geq 1$) may be cast in the form

$$i\frac{\partial \mathbf{a}^{(k)}}{\partial T_0} = -i\frac{\partial \mathbf{A}}{\partial T_k} + \mathbf{G}^{(k)}, \tag{21}$$

where $\mathbf{G}^{(k)}$ depends on functions of previous approximations. In particular, one has

$$\mathbf{G}^{(1)} = \mathcal{A}^{(0)}\mathbf{A} + \mathcal{B}\mathbf{A}, \tag{22}$$

$$\mathbf{G}^{(2)} = -i\frac{\partial \mathbf{a}^{(1)}}{\partial T_1} + \mathcal{B}\mathbf{a}^{(1)} + \mathcal{A}^{(0)}\mathbf{a}^{(1)} + \mathcal{A}^{(1)}\mathbf{A}, \tag{23}$$

$$\mathbf{G}^{(3)} = -i\frac{\partial \mathbf{a}^{(2)}}{\partial T_1} - i\frac{\partial \mathbf{a}^{(1)}}{\partial T_2} + \mathcal{B}\mathbf{a}^{(2)} + \mathcal{A}^{(0)}\mathbf{a}^{(2)} + \mathcal{A}^{(1)}\mathbf{a}^{(1)} + \mathcal{A}^{(2)}\mathbf{A}. \tag{24}$$

To avoid the occurrence of secular growing terms in the solution $\mathbf{a}^{(k)}$ to Eq. (21), which would prevent asymptotic expansion (14) to be uniformly valid in time, the following solvability condition must be satisfied:

$$i\frac{\partial \mathbf{A}}{\partial T_k} = \overline{\mathbf{G}^{(k)}}, \tag{25}$$

where the overline denotes the time average with respect to the fast time variable T_0. The solution at order $\sim\epsilon^k$ is then given by

$$\mathbf{a}^{(k)} = -i\int_0^{T_0} dt(\mathbf{G}^{(k)} - \overline{\mathbf{G}^{(k)}}). \tag{26}$$

Therefore, the solvability condition at order $\sim\epsilon^k$ determines the evolution of amplitude $\mathbf{A}$ on the slow time scale T_k; the correction to the solution $\mathbf{a}$ of order ϵ^k is then calculated using Eq. (26). By iteration, one can thus determine the temporal evolution of the amplitude $\mathbf{A}$ up to any desired scale. Note that the driving term $\mathbf{G}^{(k)}$ at any order ϵ^k can be cast in the form

$$\mathbf{G}^{(k)} = \mathcal{R}^{(k)}(T_0)\mathbf{A}, \tag{27}$$

where

$$\mathcal{R}^{(k)}(T_0) \equiv \sum_l \mathcal{R}_l^{(k)} \exp(-ilT_0) \tag{28}$$

is a periodic matrix in time with period 2π, which solely depends on matrices $\mathcal{A}^{(0)}, \mathcal{A}^{(1)}, \ldots, \mathcal{A}^{(k-1)}$, and $\mathcal{B}$. Therefore, solvability condition (25) takes the form

$$i\frac{\partial \mathbf{A}}{\partial T_k} = \mathcal{R}_0^{(k)}\mathbf{A} \tag{29}$$

and, according to Eq. (26), the solution at order $\sim\epsilon^k$ is given by

$$\mathbf{a}^{(k)} = \sum_{l \neq 0} \frac{\exp(-ilT_0) - 1}{l} \mathcal{R}_l^{(k)}\mathbf{A}. \tag{30}$$

The matrices $\mathcal{R}^{(k)}$ for the three lowest orders $k = 1, 2, 3$, which are calculated from Eqs. (22)–(24), are explicitly given by

$$\mathcal{R}^{(1)} = \mathcal{A}^{(0)} + \mathcal{B}, \tag{31}$$

$$\mathcal{R}^{(2)} = \mathcal{A}^{(1)} + \sum_{l \neq 0} \frac{\exp(-ilT_0) - 1}{l} [\mathcal{R}^{(1)}\mathcal{R}_l^{(1)} - \mathcal{R}_l^{(1)}\mathcal{R}_0^{(1)}], \tag{32}$$

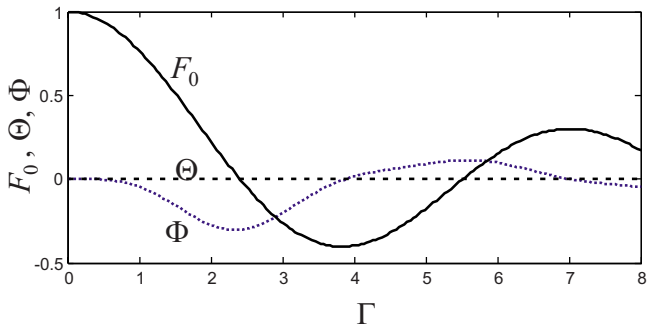

FIG. 2. (Color online) Behavior of parameters F_0, Θ, and Φ for a sinusoidal electric field with $\varphi=0$ phase versus the dimensionless parameter $\Gamma=ed\mathcal{E}_0/\hbar\omega$.

$$\mathcal{R}^{(3)} = \mathcal{A}^{(2)} + \sum_{l\neq 0} \frac{\exp(-ilT_0)-1}{l}[\mathcal{A}^{(1)}\mathcal{R}_l^{(1)} + \mathcal{R}^{(1)}\mathcal{R}_l^{(2)} - \mathcal{R}_l^{(1)}\mathcal{R}_0^{(2)} - \mathcal{R}_l^{(2)}\mathcal{R}_0^{(1)}]. \tag{33}$$

Taking into account that $d/dt=\omega(\partial_{T_0}+\epsilon\partial_{T_1}+\epsilon^2\partial_{T_2}+\cdots)$, from Eq. (29), it follows that the temporal evolution of amplitude $\mathbf{A}$ is given by

$$i\frac{d\mathbf{A}}{dt} = \epsilon\omega[\mathcal{R}_0^{(1)} + \epsilon\mathcal{R}_0^{(2)} + \epsilon^2\mathcal{R}_0^{(3)} + \cdots]\mathbf{A}. \tag{34}$$

Note that, since at any order $k\geq 1$, one has $\mathbf{a}^{(k)}=0$ for $t'=2\pi$ [see Eq. (30)], the quasienergies E_l of the original system (9) are given by $E_l=\hbar\omega\epsilon\lambda_l$, where λ_l are the eigenvalues of the matrix

$$\mathcal{R} \equiv \mathcal{R}_0^{(1)} + \epsilon\mathcal{R}_0^{(2)} + \epsilon^2\mathcal{R}_0^{(3)} + \cdots. \tag{35}$$

The averaging method of Sec. II B corresponds to stopping the asymptotic analysis up to first order. In fact, in this case, one has $\mathcal{R}\simeq\mathcal{R}_0^{(1)}=\overline{\mathcal{M}(t')}$. It is obvious that, to safely describe the temporal evolution of original Eq. (9) and thus the corresponding behavior of quasienergies, the asymptotic analysis should be pushed up to the minimum order k such that $\mathcal{R}_0^{(k)}$ does not identically vanish. Depending on amplitude and frequency of the applied electric field, we must therefore distinguish two cases.

(i) *First case: Electric field amplitude tuned far from a quasienergy collapse point.* This case is met whenever $F_0\sim O(1)$, i.e., $\mathcal{A}^{(0)}\neq 0$. For a sinusoidal field [Eq. (7)], this condition is satisfied for a field amplitude $\mathcal{E}_0$ such that $J_0(ed\mathcal{E}_0/\hbar\omega)$ is of order ~ 1. Since in this case $\mathcal{R}_0^{(1)}=\mathcal{A}^{(0)}\neq 0$ [see Eq. (17)], the first-order term in Eq. (34) is enough to capture the temporal dynamics of tunneling, i.e., one can safely apply the averaging method of Sec. II B.

(ii) *Second case: Electric field amplitude tuned near a quasienergy collapse point.* In this case, which corresponds to a small value of F_0 (of order $\sim\epsilon$ or smaller), one has $\mathcal{R}_0^{(1)}=0$ and therefore the asymptotic analysis should be pushed at the next order $\sim\epsilon^2$ since $\partial_{T_1}\mathbf{A}=0$. From Eq. (32) with $\mathcal{A}^{(0)}=0$, it follows that

$$\mathcal{R}^{(2)} = \mathcal{A}^{(1)} + \sum_{l,m\neq 0}\left(\frac{\exp(-ilT_0)-1}{l}\right)\exp(-imT_0)\mathcal{B}_m\mathcal{B}_l, \tag{36}$$

where we have set $\mathcal{B}(T_0)\equiv\Sigma_{l\neq 0}\mathcal{B}_l\exp(-ilT_0)$. The dc value $\mathcal{R}_0^{(2)}$ of $\mathcal{R}^{(2)}$ is hence

$$\mathcal{R}_0^{(2)} = \mathcal{A}^{(1)} + \sum_{l\neq 0}\frac{\mathcal{B}_{-l}\mathcal{B}_l}{l}. \tag{37}$$

Taking into account the expressions of $\mathcal{A}$ and $\mathcal{B}(T_0)$ given by Eqs. (17) and (18), after some algebra from Eq. (37), one then obtains

$$(\mathcal{R}_0^{(2)})_{n,m} = -\Theta(\theta_n^2-\theta_{n-1}^2)\delta_{n,m} + \theta_n F_0^{(1)}\delta_{n,m-1} + \theta_{n-1}F_0^{(1)*}\delta_{n,m+1}, \tag{38}$$

where we have set

$$\Theta \equiv \sum_{l\neq 0}\frac{|F_l|^2}{l}. \tag{39}$$

Taking into account that $\Delta_n=\epsilon\theta_n\omega$ and $\epsilon F_0^{(1)}=F_0$, the coupled equations for the slow evolution of amplitudes A_n [Eq. (34)] up to the time scale $\sim 1/\epsilon^2$ are thus given by

$$i\frac{dA_n}{dt} = -\frac{\Theta}{\omega}(\Delta_n^2-\Delta_{n-1}^2)A_n + F_0\Delta_n A_{n+1} + F_0^*\Delta_{n-1}A_{n-1}. \tag{40}$$

Such equations, which are accurate up to the time scale $\sim 1/\epsilon^2$, have been previously derived in Ref. 17. Note that, for a driving field such that $\Theta\neq 0$ and for a truncated array, the matrix $\mathcal{R}_0^{(2)}$ is always nonvanishing, even if F_0 vanishes, and therefore Eq. (40) give an accurate description of the tunneling dynamics *even* when the collapse point is crossed. Such a condition is satisfied, for instance, for a bichromatic electric field (the case considered in Ref. 17). However, for a sinusoidal field [Eq. (7)], one has $\Theta=0$, and therefore Eq. (40) fails to describe the tunneling dynamics when $F_0^{(1)}=0$, i.e., very close to the collapse point, since in this case one has $\partial_{T_2}A_n=0$ and the tunneling dynamics occurs on the longer time scale $T_3\sim 1/\epsilon^3$. Such a situation is precisely the one corresponding to selective CDT investigated in Ref. 18, which requires therefore to push the perturbative analysis up to order $\sim\epsilon^3$.

For $\Theta=0$ and $F_0^{(0)}=F_0^{(1)}=0$, one needs to calculate the dc value of $\mathcal{R}^{(3)}$. From Eq. (33) with $\mathcal{A}^{(0)}=\mathcal{A}^{(1)}=\mathcal{R}_0^{(2)}=0$, one obtains

$$\mathcal{R}^{(3)} = \mathcal{A}^{(2)} + \sum_{l\neq 0}\left(\frac{\exp(-ilT_0)-1}{l}\right)\mathcal{B}\mathcal{R}_l^{(2)}. \tag{41}$$

The expressions of $\mathcal{R}_l^{(2)}$ can be easily calculated from Eq. (32),

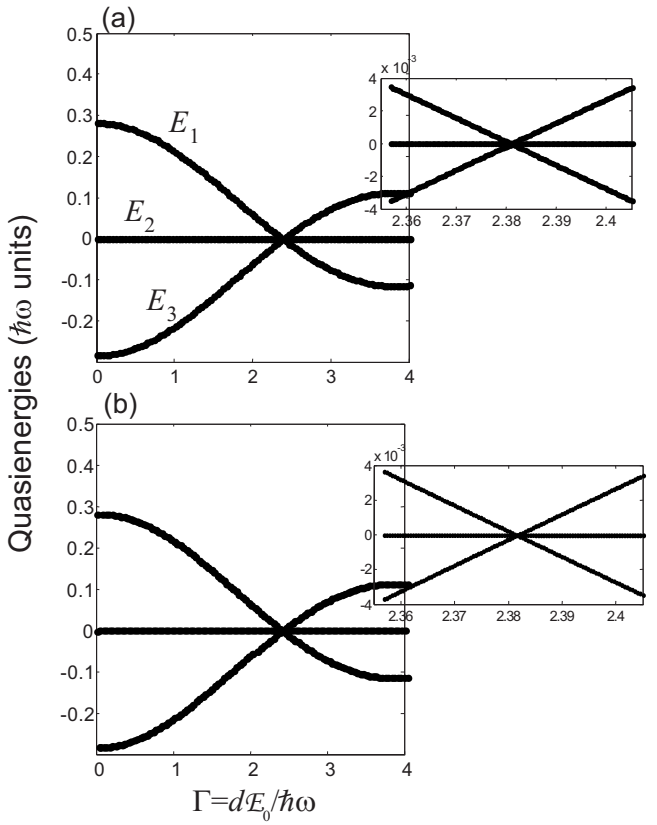

FIG. 3. Behavior of quasienergies E_l (in units $\hbar\omega$) versus $\Gamma = ed\mathcal{E}_0/\hbar\omega$ in a triple-well chain driven by a sinusoidal electric field as predicted (a) by numerical analysis of original Eq. (4) and (b) by the perturbative analysis [Eq. (60)] for $\Delta/\omega = 0.2$. The insets show an enlargement of quasienergies near the collapse point $\Gamma = 2.405$, corresponding to the first zero of Bessel J_0 function.

$$\mathcal{R}_l^{(2)} = \sum_{m\neq 0} \frac{-\mathcal{B}_l\mathcal{B}_m + \mathcal{B}_{l-m}\mathcal{B}_m}{m}. \tag{42}$$

From Eqs. (41) and (42) and taking into account that $\Sigma_{l\neq 0}\mathcal{B}_l\mathcal{B}_{-l}/l = 0$, one readily obtains

$$\mathcal{R}_0^{(3)} = \mathcal{A}^{(2)} + \sum_{m,l\neq 0} \frac{\mathcal{B}_{-l}\mathcal{B}_{l-m}\mathcal{B}_m}{lm}. \tag{43}$$

Taking into account the expressions of $\mathcal{A}$ and $\mathcal{B}(T_0)$ given by Eqs. (17) and (18), after some algebra from Eq. (43), one then obtains

$$\begin{aligned}(\mathcal{R}_0^{(3)})_{n,m} = {} & [\theta_n F_0^{(2)} - \Phi(\theta_n\theta_{n+1}^2 - 2\theta_n^3 + \theta_n\theta_{n-1}^2)]\delta_{n,m-1} \\ & + [\theta_{n-1}F_0^{(2)*} - \Phi^*(\theta_n^2\theta_{n-1} - 2\theta_{n-1}^3 \\ & + \theta_{n-1}\theta_{n-2}^2)]\delta_{n,m+1},\end{aligned} \tag{44}$$

where we have set

$$\Phi \equiv -\sum_{l,j\neq 0} \frac{F_l F_j^* F_{j-l}}{lj}. \tag{45}$$

Finally, taking into account that $\Delta_n = \epsilon\theta_n\omega$ and $\epsilon^2 F_0^{(2)} = F_0$, the coupled equations for the slow evolution of amplitudes A_n [Eq. (34)] up to the time scale $\sim 1/\epsilon^3$ are thus given by

$$\begin{aligned}i\frac{dA_n}{dt} = {} & \left[\Delta_n F_0 - \frac{\Phi}{\omega^2}(\Delta_n\Delta_{n+1}^2 - 2\Delta_n^3 + \Delta_n\Delta_{n-1}^2)\right]A_{n+1} \\ & + \left[\Delta_{n-1}F_0^* - \frac{\Phi^*}{\omega^2}(\Delta_{n-1}\Delta_n^2 - 2\Delta_{n-1}^3 + \Delta_{n-1}\Delta_{n-2}^2)\right]A_{n-1}.\end{aligned} \tag{46}$$

Equation (46) describes the tunneling dynamics up to the time scale $1/\epsilon^3$ near the collapse point for $F_0 \sim \epsilon^2$ in case $\Theta = 0$. It should be noted that, for a finite chain, $\mathcal{R}_0^{(3)}$ does not identically vanish when crossing the collapse point, i.e., for $F_0 = 0$, because it is likely that $\Phi \neq 0$. This occurs, as an example, for a sinusoidal electric field [Eq. (7)], which is of major interest in applications. In this case, the behavior of both F_0 and Φ versus the dimensionless parameter $\Gamma = ed\mathcal{E}_0/\hbar\omega$ is plotted in Fig. 2, showing that at the zeros of F_0, one has $\Phi \neq 0$. The amplitude equation, given by Eq. (26) is therefore expected to be accurate enough to predict the main features of tunneling dynamics in a finite chain driven by a sinusoidal electric field, such as selective CDT numerically predicted in Ref. 18. This will be shown in detail in Sec. IV.

To summarize, we may conclude that the solution to original Eq. (4) in the large-frequency limit can be written as $a_n(t) = A_n(t) + O(\epsilon)$, where the temporal evolution of amplitudes $A_n(t)$ up to the time scale $\sim 1/\epsilon^3$ is ruled by the autonomous system

$$\begin{aligned}i\frac{dA_n}{dt} = {} & -\theta(\Delta_n^2 - \Delta_{n-1}^2)A_n + [\Delta_n F_0 - \phi(\Delta_n\Delta_{n+1}^2 - 2\Delta_n^3 \\ & + \Delta_n\Delta_{n-1}^2)]A_{n+1} + [\Delta_{n-1}F_0^* - \phi^*(\Delta_{n-1}\Delta_n^2 - 2\Delta_{n-1}^3 \\ & + \Delta_{n-1}\Delta_{n-2}^2)]A_{n-1}.\end{aligned} \tag{47}$$

In Eq. (47), the constants θ and ϕ are given by

$$\theta = \frac{\Theta}{\omega} = \sum_{l\neq 0} \frac{|F_l|^2}{l\omega}, \phi = \frac{\Phi}{\omega^2} = -\sum_{l,j\neq 0} \frac{F_l F_j^* F_{j-l}}{\omega^2 lj} \tag{48}$$

and F_l are the Fourier expansion coefficients defined by Eq. (6). The Floquet exponents (quasienergies) μ_l of original problem (4) should be thus approximated by the eigenvalues of the matrix $\mathcal{R}$ associated with system (47), even close to a quasienergy pseudocollapse point, with an accuracy of order ϵ^3.

We finally note that the previous analysis, which leads to Eq. (47), holds provided that, according to model (1), all localized states $|n\rangle$ in the chain have the same energy in the absence of the external driving field. Such a condition, however, may not be exactly satisfied owing to, e.g., boundary effects of the potential. Slight shifts $\hbar\delta\omega_n$ of the energy levels for the localized states $|n\rangle$ from a reference level—of the order of $\hbar\Delta_n$ or smaller—might be included in the analysis, if needed, by adding the terms $\delta\omega_n A_n$ on the right hand sides in Eq. (47). For the sake of simplicity, in the following, we will assume $\delta\omega_n = 0$.

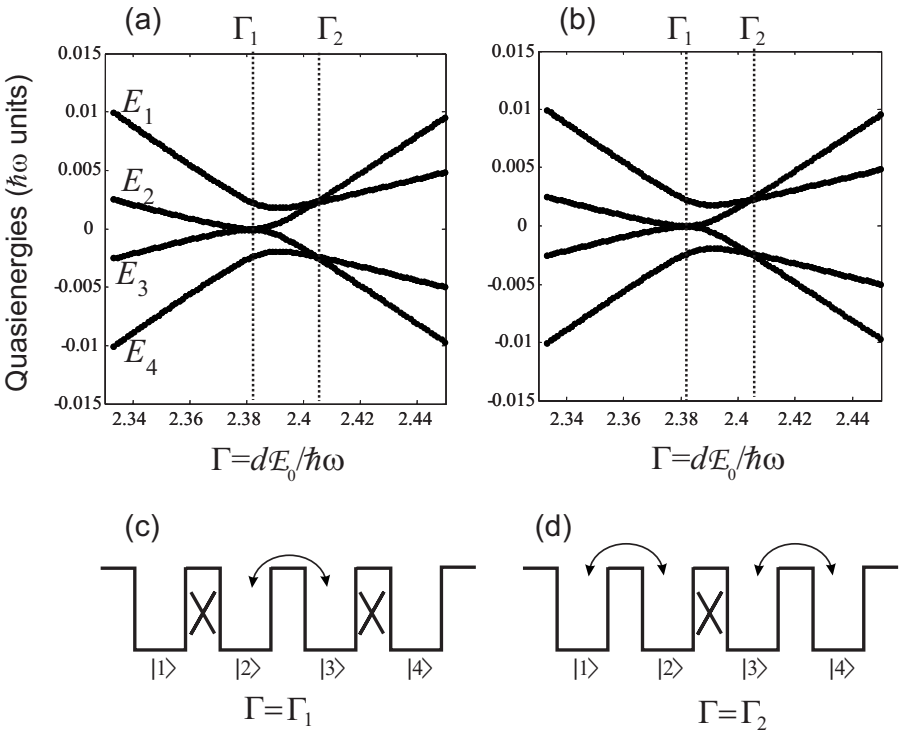

FIG. 4. [(a) and (b)] Behavior of quasienergies E_l (in units $\hbar\omega$) versus $\Gamma = ed\mathcal{E}_0/\hbar\omega$ in a chain of $N=4$ wells near the first collapse region as predicted (a) by numerical analysis of original Eq. (4) and (b) by the third-order perturbative analysis for $\Delta/\omega = 0.2$. Lower panels in (c) and (d) are schematic representations of the tunneling dynamics in the chain when the field amplitude is tuned (c) at the anticrossing point $\Gamma = \Gamma_1$ and (d) at the crossing point $\Gamma = \Gamma_2$. Crosses indicate suppression of tunneling through that barrier, whereas the arrows indicate that tunneling is allowed.

IV. APPLICATION OF THE PERTURBATIVE THEORY TO TUNNELING CONTROL

In this section, the results of the third-order perturbation analysis, summarized by Eq. (47), are applied to describe the main features of tunneling dynamics in a NNTB chain driven by an ac electric field composed by a few coupled quantum wells. In particular, we will show that selective CDT recently proposed in Ref. 18 in the framework of a nonperturbative theory is captured by the perturbative theory and is consistent with the behavior of quasienergies near the collapse point according to the generalized symmetries of the Floquet states.

Let us consider a chain made of N wells with equal hopping rates Δ (i.e., $\Delta_n = \Delta$ for $n = 1, 2, \ldots, N-1$, $\Delta_n = 0$ otherwise), and let us assume a sinusoidal electric field with frequency ω, amplitude $\mathcal{E}_0$, and phase $\varphi = 0$ [see Eq. (7)]. In correspondence, one has $\Theta = 0$ and

$$F_0 = J_0(\Gamma), \quad \phi = -\frac{1}{\omega^2} \sum_{l,j \neq 0} \frac{J_l(\Gamma) J_j(\Gamma) J_{j-l}(\Gamma)}{lj}. \tag{49}$$

where

$$\Gamma \equiv \frac{ed\mathcal{E}_0}{\hbar\omega}. \tag{50}$$

It should be noted that a different choice of the phase φ of the electric field does not obviously change the quasienergy spectrum and thus the tunneling dynamics at long time scales, although it may change the tunneling probability over one modulation cycle.[25]

A. Generalized parity, level crossings, and avoided crossings

The quasienergies E_l of the multiple-well system are usually intricate functions of the electric field amplitude $\mathcal{E}_0$ and undergo a series of apparent crossings and avoided crossings when $\mathcal{E}_0$ is varied near the collapse point, according to the generalized (or dynamical) symmetries of the Floquet states (see, for instance, Refs. 6 and 26–29). The precise determination of such crossings and avoided crossings is a rather formidable task, especially as the number N of wells (and hence the number of nearly degenerate quasienergies that interact near the collapse point) increases. A full numerical computation of the system propagator over one modulation cycle (as done, for instance, in Ref. 18) is therefore in order. Nevertheless, for a driving field $E(t)$ such that $E(t+T/2) = -E(t)$, where $T = 2\pi/\omega$ is the modulation period, some general results can be stated on the basis of the generalized symmetries of the Floquet states that follow from the invariance of the problem to the simultaneous temporal translation $t \to t+T/2$ and spatial reflection $x \to -x$, as discussed in Appendix A. In particular, the following properties can be demonstrated.

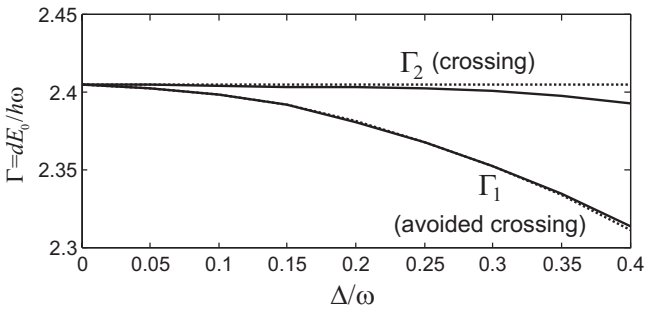

FIG. 5. Behavior of normalized field amplitudes Γ_1 (for level avoided crossing) and Γ_2 (for level crossing) versus Δ/ω in a $N=4$ chain. The solid curves refer to nonperturbative results; the dotted curves refer to the results obtained by the perturbative analysis [Eqs. (61)–(64)].

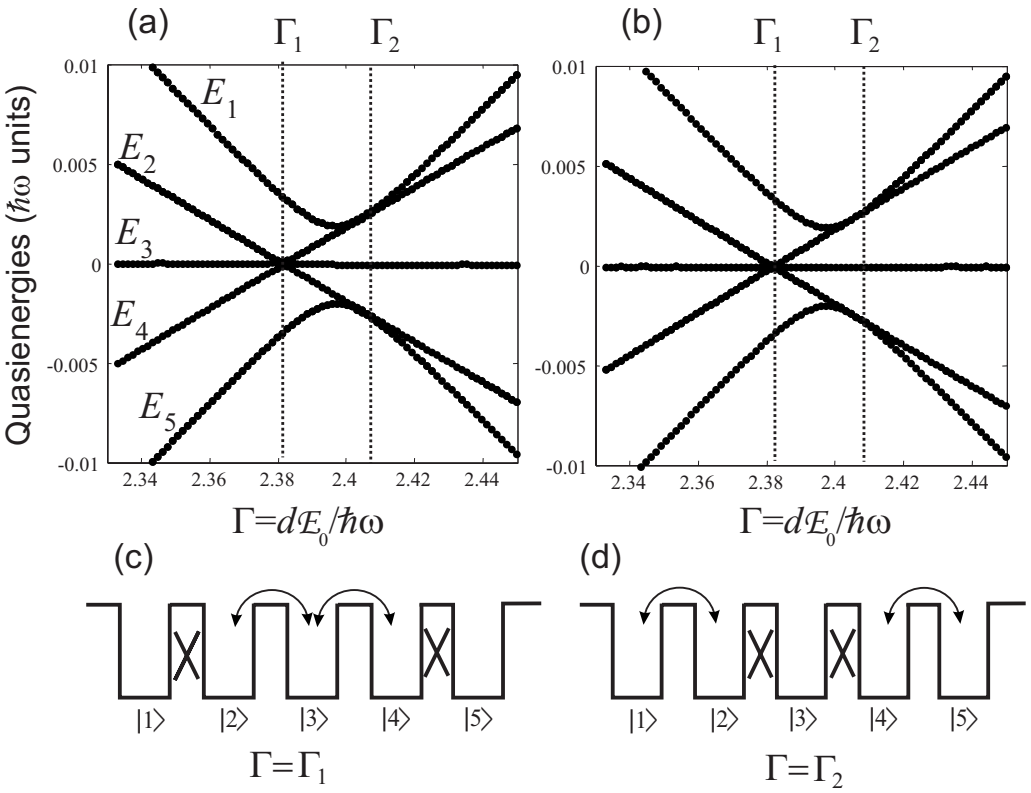

FIG. 6. Same as Fig. 4, but for a chain made of $N=5$ wells.

(i) *Generalized parity of Floquet states*. Let $\psi_l \equiv u_n^{(l)}(t)$ be the periodic part of a Floquet state corresponding to the quasienergy $E_l=\hbar\mu_l$. Then, ψ_l has a well-defined (generalized) parity for the combined discrete spatial reflection $n \to N-n+1$ and time translation $t \to t+T/2$, i.e., one always has

$$u_{N-n+1}^{(l)}(t+T/2) = u_n^{(l)}(t) \quad \text{(even parity state)} \tag{51}$$

or

$$u_{N-n+1}^{(l)}(t+T/2) = -u_n^{(l)}(t) \quad \text{(odd parity state)}. \tag{52}$$

(ii) *Distribution of quasienergies*. Let $\psi_l \exp(-i\mu_l t) = u_n^{(l)}(t)\exp(-i\mu_l t)$ be a Floquet state of Eq. (4) corresponding to the quasienergy $E_l=\hbar\mu_l$. Then, $(-1)^n u_{N-n+1}^{(l)*}(t)\exp(i\mu_l t)$ is also a Floquet state for Eq. (4) with quasienergy $-E_l$. We can then order the N Floquet states of Eq. (4) in such a way that

$$E_{N-l+1} = -E_l, \quad u_n^{(N-l+1)}(t) = (-1)^n u_{N+1-n}^{(l)*}(t) \tag{53}$$

for $l=1,2,3,\ldots,N$. Note, in particular, that for an odd number N of wells, one has $E_{(N+1)/2}=0$, i.e., there always exists a Floquet state with zero quasienergy.

(iii) *Connection between the quasienergies and the energies of the undriven system*. When the driving field amplitude is adiabatically switched off ($\mathcal{E}_0 \to 0$), the Floquet states and corresponding quasienergies are connected with the stationary eigenfunctions and corresponding energies of Eq. (4) as follows:

$$u_n^{(l)}(t) \to \sqrt{\frac{2}{N+1}} \sin\left(\frac{nl\pi}{N+1}\right) \exp(im_l\omega t),$$

$$E_l(\mathcal{E}_0) \to 2\hbar\Delta \cos\left(\frac{l\pi}{N+1}\right) - m_l\hbar\omega \ (\mathcal{E}_0 \to 0) \tag{54}$$

($l=1,2,3,\ldots,N$), where m_l is a suitable integer that counts "how many photons" have to be subtracted from the undriven energy level in order to push the quasienergy E_l in the first Brillouin zone. Note that $m_l=0$ for $2\Delta < \omega/2$. Such a property is helpful to determine the generalized parity of the Floquet states. In particular, note that for $\omega > 4\Delta$, the Floquet state $\psi_l \exp(-i\mu_l t)$ has a generalized even parity for l odd and a generalized odd parity for l even.

The dynamical symmetries of the Floquet states, as well as the property (ii) cited above, play an important role in determining the behavior of crossings and avoided crossings of quasienergies near the collapse point $\Gamma \sim 2.4$. For instance, according to the von Neumann–Wigner theorem,[30] it is well known that the approaching of quasienergies of two Floquet states with opposite generalized parity yields an exact crossing, whereas the approaching of quasienergies of two Floquet states with the same parity yields an avoided crossing (see, for instance, Ref. 6). Such a scenario becomes more involved when there is a simultaneous collapse of more than two quasienergies, which is the case of our multiple-well system for $N \geq 3$ near $\Gamma \sim 2.4$ in the large-frequency limit. Even though the exact form of the Floquet states is not known, the peculiar behavior of multilevel crossings and anticrossings for the $N \geq 3$ quasienergies near $\Gamma \sim 2.4$ can be derived by a simple extension of the argument proposed by Landau and Lifshitz[31] for the problem of level crossing or

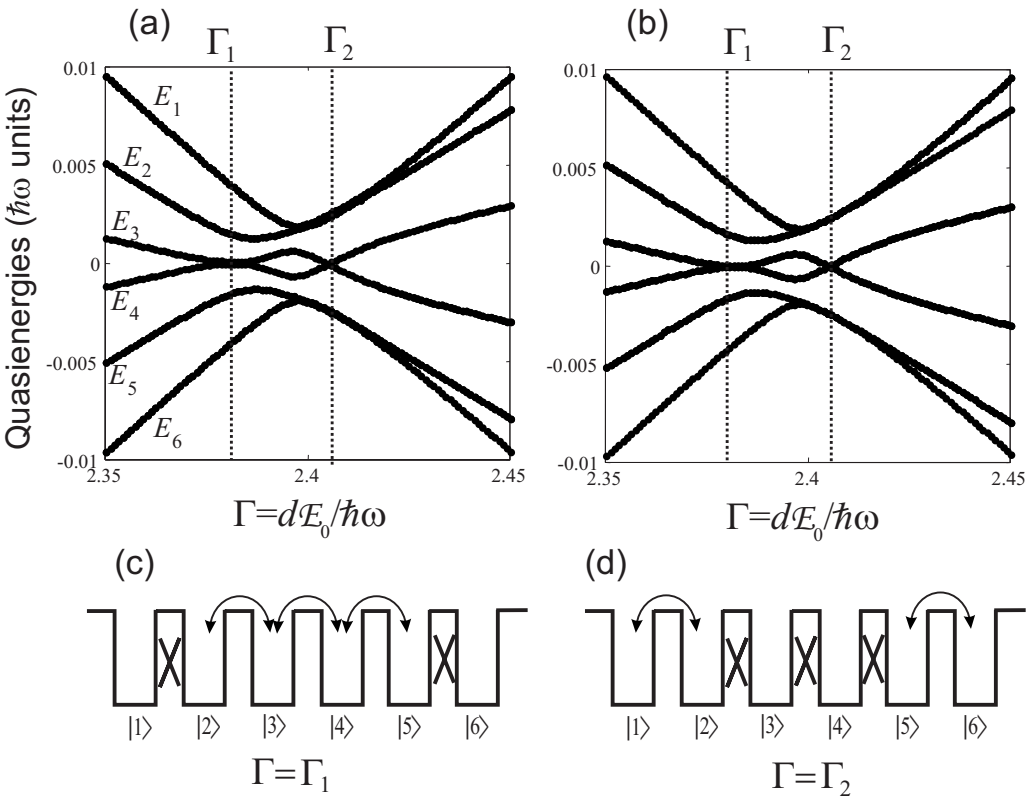

FIG. 7. Same as Fig. 4, but for a chain made of $N=6$ wells.

avoided crossing for the two states. Such an analysis is presented in Appendix B. Here, we just mention that the scenario of quasienergy crossings and/or avoided crossings for $N=3$, 4, wells predicted by the perturbative analysis up to third order [Eq. (47)] and shown in Figs. 3–7 (to be discussed in Secs. IV C and IV D) is consistent with the results based on the dynamical symmetries of the Floquet states.

B. Coherent destruction of tunneling in a double-well system

The simplest case is that of a chain composed by $N=2$ wells, which has been extensively studied in the literature (see, for instance, Refs. 12, 13, 15, 16, and 22). In this case, Eq. (47) explicitly reads

$$i\frac{dA_1}{dt} = \Delta(F_0 + 2\Delta^2\phi)A_2,\ i\frac{dA_2}{dt} = \Delta(F_0 + 2\Delta^2\phi)A_1. \tag{55}$$

The quasienergies, calculated from Eq. (55), are given by

$$E_{1,2}(\Gamma) = \pm\hbar\Delta(F_0 + 2\Delta^2\phi). \tag{56}$$

CDT corresponds to crossing of quasienergies, i.e., to $E_1 = E_2 = 0$, which is attained at $F_0 + 2\Delta^2\phi = 0$. Note that, as compared to the usual large-frequency limit based on the averaging technique,[12,13] a third-order correction to the quasienergies appears in Eq. (56), which is in agreement with the previous refined analyses for strongly driven two-level systems.[15,22] As such a problem has been widely investigated in the literature, it will not be discussed here further.

C. Coherent destruction of tunneling in a triple-well system

Let us consider now a triple-well system, for which Eq. (47) takes the explicit form

$$i\frac{dA_1}{dt} = \Delta(F_0 + \Delta^2\phi)A_2, \tag{57}$$

$$i\frac{dA_2}{dt} = \Delta(F_0 + \Delta^2\phi)(A_1 + A_3), \tag{58}$$

$$i\frac{dA_3}{dt} = \Delta(F_0 + \Delta^2\phi)A_2. \tag{59}$$

The quasienergies calculated from the approximate [Eqs. (57)–(59)] are then given by

$$E_1 = \sqrt{2}\hbar\Delta(F_0 + \Delta^2\phi),\ E_2 = 0,\ E_3 = -E_1. \tag{60}$$

Note that an exact crossing of quasienergies, which corresponds to CDT, is attained for $F_0 + \Delta^2\phi = 0$. Such a result is in agreement with the predictions based on the dynamical symmetries of the Floquet states, as shown in Appendix B [see Eq. (B10)]. A comparison of the quasienergies predicted by Eq. (60) and by a direct numerical integration of original Eq. (4) using an accurate variable-step fourth-order Runge method is reported in Fig. 3 for $\Delta/\omega = 0.2$. Note the good agreement between the curves, which includes the prediction of a shift of Γ from the 2.405 root of the Bessel function J_0 to achieve CDT (see the insets of Fig. 3).

D. Selective coherent destruction of tunneling in a chain with $N=4,5$, and 6 wells

In this section, we specialize Eq. (47) to study selective CDT in arrays made of $N=4,5$, or 6 wells, which is closely related to the existence of crossings and avoided crossings of quasienergies near the collapse point $\Gamma=2.405$ according to the dynamical symmetries of the Floquet states, as discussed in Appendix B.

Consider first the case $N=4$. The evolution equations for the slowly varying amplitudes A_n [Eq. (47)] explicitly read

$$i\frac{dA_1}{dt} = \Delta(F_0 + \Delta^2\phi)A_2, \tag{61}$$

$$i\frac{dA_2}{dt} = \Delta(F_0 + \Delta^2\phi)A_1 + \Delta F_0 A_3, \tag{62}$$

$$i\frac{dA_3}{dt} = \Delta F_0 A_2 + \Delta(F_0 + \Delta^2\phi)A_4, \tag{63}$$

$$i\frac{dA_4}{dt} = \Delta(F_0 + \Delta^2\phi)A_3. \tag{64}$$

The four eigenvalues λ_l associated with Eqs. (61)–(64) are the roots of the following quadratic equation in λ^2:

$$\lambda^4 - [\Delta^2 F_0^2 + 2\Delta^2(F_0 + \Delta^2\phi)^2]\lambda^2 + \Delta^4(F_0 + \Delta^2\phi)^4 = 0. \tag{65}$$

A typical behavior of quasienergies $E_l=\hbar\lambda_l$ near the collapse point $\Gamma\sim 2.4$, which is predicted by the perturbative analysis, is plotted in Fig. 4(b) and compared to that obtained by a numerical computation of the one-period propagator for original time-periodic Eq. (4) [Fig. 4(a)]. The value of Δ/ω chosen in Fig. 4(a) is 0.2 and thus corresponds to the condition of Figs. 1–3 of Ref. 18. An inspection of Eq. (65), which has the same structure of Eq. (B11) given in Appendix B and derived on the basis of dynamical symmetries of the Floquet states, indicates that the quasienergies E_2 and $E_3=-E_2$ undergo an avoided crossing at $\Gamma=\Gamma_1$, whereas crossing for pairs of quasienergies E_1, E_2 and E_3, E_4 occurs at $\Gamma=\Gamma_2$ [see Fig. 4(a)]. The behavior of Γ_1 and Γ_2 versus Δ/ω, which is calculated by the perturbative theory, is plotted in Fig. 5 and compared to the one obtained by a full numerical analysis of Eq. (4) (see also Fig. 4 of Ref .18). Note the good agreement between the curves, at least for $\Delta/\omega<0.25$. In the perturbative analysis, the value of Γ_1 (level avoided crossing) corresponds to $F_0+\Delta^2\phi=0$, at which one has $E_2=E_3=0$ and $E_1=-E_4=\hbar\Delta F_0$. The value of Γ_2, which corresponds to a pair of quasienergy crossings, is attained when $F_0=0$, i.e., one has $\Gamma_2=2.405$ independently of Δ/ω (see Fig. 5). Selective CDT discussed in Ref. 18 and schematized in Figs. 4(c) and 4(d) can be easily understood in the framework of the perturbative analysis by an inspection of Eqs. (61)–(64). Let us first consider the anticrossing point $\Gamma=\Gamma_1$. In this case, one has $F_0+\Delta^2\phi=0$, and thus from Eqs. (61) and (64), one obtains $dA_1/dt=dA_4/dt=0$: this means that at $\Gamma=\Gamma_1$ suppression of tunneling for an electron initially prepared in either wells 1 or 4 is attained [see Fig. 4(c)]. Conversely, Eqs. (62) and (63) show that a nonvanishing tunneling probability persists for an electron initially prepared in either wells 2 or 3. For example, if an electron is initially prepared in well 2, the occupation probabilities $P_2(t)=|A_2(t)|^2$ and $P_3(t)=|A_3(t)|^2$ of wells 2 and 3 undergo Rabi-type oscillations according to

$$P_2(t) = \cos^2(\Delta_{\rm eff}t),\ P_3(t) = \sin^2(\Delta_{\rm eff}t), \tag{66}$$

with an effective tunneling rate $\Delta_{\rm eff}$ given by

$$\Delta_{\rm eff} = \Delta F_0 = -\Phi(\Gamma_1)\Delta\left(\frac{\Delta}{\omega}\right)^2. \tag{67}$$

Note that, from the plot of the function $\Phi(\Gamma)$ depicted in Fig. 2, one has $\Phi(\Gamma_1)\sim -0.3$, and therefore the effective tunneling rate $\Delta_{\rm eff}$ is reduced as compared to its value Δ in the undriven case by a factor $\sim 0.3(\Delta/\omega)^2$. Let us then consider the crossing point $\Gamma=\Gamma_2$. In this case, from Eqs. (61)–(64), it follows that the dynamics of A_1, A_2 decouples from that of A_3,A_4, i.e., the dynamical scenario depicted in Fig. 4(d) is attained according to the analysis of Ref. 18. For instance, if an electron is initially prepared in well 1 or in well 2, the occupation probabilities $P_1(t)=|A_1(t)|^2$ and $P_2(t)=|A_2(t)|^2$ undergo Rabi-type oscillations, whereas the occupation probabilities of wells 3 and 4 remain zero. According to Eqs. (61) and (62), the effective tunneling rate $\Delta_{\rm eff}$ of such Rabi flopping is given by $\Delta_{\rm eff}=\Phi(\Gamma_2)\Delta(\Delta/\omega)^2$, which should be compared to that obtained for the $\Gamma=\Gamma_1$ tuning condition [Eq. (67)]. As $\Phi(\Gamma_1)\simeq\Phi(\Gamma_2)\simeq -0.3$ for Γ_1 and Γ_2 near $\sim 2.3-2.4$, we may conclude that, apart from a sign reversal, the effective tunneling rate (and thus the period of Rabi-type oscillations) is approximately the same for the avoided crossing ($\Gamma=\Gamma_1$) and crossing ($\Gamma=\Gamma_2$) tuning conditions.

The above analysis can be extended to chains made of $N=5$ or $N=6$ wells. For $N=5$, the evolution equations for the slowly varying amplitudes A_n [Eq. (47)] explicitly read

$$i\frac{dA_1}{dt} = \Delta(F_0 + \Delta^2\phi)A_2, \tag{68}$$

$$i\frac{dA_2}{dt} = \Delta(F_0 + \Delta^2\phi)A_1 + \Delta F_0 A_3, \tag{69}$$

$$i\frac{dA_3}{dt} = \Delta F_0 A_2 + \Delta F_0 A_4, \tag{70}$$

$$i\frac{dA_4}{dt} = \Delta F_0 A_3 + \Delta(F_0 + \Delta^2\phi)A_5, \tag{71}$$

$$i\frac{dA_5}{dt} = \Delta(F_0 + \Delta^2\phi)A_4. \tag{72}$$

A typical behavior of quasienergies E_l near the collapse point $\Gamma\sim 2.4$, which is predicted by the perturbative analysis, is plotted in Fig. 6(b) and compared to that obtained by a numerical nonperturbative analysis [Fig. 6(a)]. In the Fig. 6(a), the schematic representations of the tunneling scenario for a field amplitude tuned at $\Gamma=\Gamma_1$ [corresponding to $F_0+\Delta^2\phi=0$; Fig. 6(c)] and at $\Gamma=\Gamma_2$ [corresponding to $F_0=0$; Fig. 6(d)] are also reported. Note that in the former case from

Eqs. (68)–(72), one obtains $dA_1/dt=dA_5/dt=0$, i.e., tunneling is suppressed for an electron initially prepared in one of the two boundary wells, whereas tunneling is allowed among wells 2, 3, and 4, with an effective tunneling rate given by Eq. (67). For an initial condition corresponding to an electron prepared in one of the three wells, 2, 3, or 4, the occupation probabilities $P_2(t)$, $P_3(t)$, and $P_4(t)$ can be analytically computed by a straightforward eigenmode analysis of Eqs. (69)–(71). For $\Gamma=\Gamma_2$, from Eq. (70), it follows that $dA_3/dt=0$, i.e., tunneling is suppressed if an electron is initially prepared in the middle well [see Fig. 6(d)].

Finally, for a chain made of $N=6$ wells, one has

$$i\frac{dA_1}{dt} = \Delta(F_0 + \Delta^2\phi)A_2, \tag{73}$$

$$i\frac{dA_2}{dt} = \Delta(F_0 + \Delta^2\phi)A_1 + \Delta F_0 A_3, \tag{74}$$

$$i\frac{dA_3}{dt} = \Delta F_0 A_2 + \Delta F_0 A_4, \tag{75}$$

$$i\frac{dA_4}{dt} = \Delta F_0 A_3 + \Delta F_0 A_5, \tag{76}$$

$$i\frac{dA_5}{dt} = \Delta F_0 A_4 + \Delta(F_0 + \Delta^2\phi)A_6, \tag{77}$$

$$i\frac{dA_6}{dt} = \Delta(F_0 + \Delta^2\phi)A_5. \tag{78}$$

A typical behavior of quasienergies E_l near the collapse point $\Gamma\sim 2.4$ is reported in Fig. 7, together with a schematic representation of the tunneling scenario for a field amplitude tuned at $\Gamma=\Gamma_1$ [corresponding to $F_0+\Delta^2\phi=0$; Fig. 7(c)] and at $\Gamma=\Gamma_2$ [corresponding to $F_0=0$; Fig. 7(d)]. Note that in the former case, tunneling is suppressed for an electron initially prepared in one of the two boundary wells, whereas in the latter case, CDT occurs for an electron initially prepared in either wells 3 or 4 (at least up to the time scale $\sim 1/\epsilon^3$).

V. CONCLUSIONS

In this work, a theoretical analysis of quantum tunneling in ac-driven tight-binding chains made of a finite number of sites, such as electronic tunneling in finite superlattices of quantum wells or in linear chains of quantum dots, has been presented in the large-frequency limit. A multiple-scale asymptotic analysis of the underlying equations in the NNTB approximation has been developed, which is exact up to the time scale $\sim 1/\epsilon^3$, where ϵ in the ratio between the characteristic tunneling hopping rate and the modulation frequency. It has been shown that the asymptotic analysis pushed up to the time scale $1/\epsilon^3$ correctly captures the main features of the tunneling process in the multiple-well structure and the complex behavior of crossings and avoided crossings of quasienergies near a collapse point, according to the dynamical symmetries of the Floquet states. An application of the perturbative analysis has been presented to explain selective CDT in ac-driven quantum-dot arrays previously proposed in Ref. 18.

APPENDIX A: GENERALIZED SYMMETRIES OF FLOQUET STATES

Let us indicate by $\psi_l=u_n^{(l)}(t)$ the periodic part of the Floquet state of Eq. (4) corresponding to the quasienergy $E_l=\hbar\mu_l$, which is assumed to be confined in the first Brillouin zone (i.e., $-\hbar\omega/2\le E_l<\hbar\omega/2$). Then, it follows that ψ_l satisfies the eigenvalue equation

$$\mathcal{H}\psi_l = E_l\psi_l, \tag{A1}$$

where the Hermitian operator $\mathcal{H}$, which is defined on the space of periodic functions with period $T=2\pi/\omega$, is given by

$$\mathcal{H} = \mathcal{M}(t) - i\hbar\frac{\partial}{\partial t} \tag{A2}$$

and

$$\mathcal{M}_{n,m}(t) = \hbar\Delta F(t)\delta_{n,m-1} + \hbar\Delta F^*(t)\delta_{n,m+1}. \tag{A3}$$

The periodic parts of the Floquet states form therefore a set of orthonormal functions, i.e.,

$$\langle\psi_l|\psi_r\rangle \equiv \sum_n \int_0^T dt\, u_n^{(l)*}(t)u_n^{(r)}(t) = \delta_{l,r}. \tag{A4}$$

For a finite chain made of N wells, the matrix $\mathcal{M}$ should be obviously truncated to define a matrix of order $N\times N$, and the sum in Eq. (A4) should be extended from $n=1$ to $n=N$, however, for the following analysis, one may equivalently use the not truncated expression [Eq. (A3)] for $\mathcal{M}$ and extend the sum in Eq. (A4) to any integer n, provided that one takes $u_n^{(l)}=0$ for $n\le 0$ and for $n\ge N+1$.

Let us now assume that the ac driving field $E(t)$ satisfies the condition $E(t+T/2)=-E(t)$, so that from Eq. (5), it follows that $F(t+T/2)=F^*(t)$. In the continuous Hamiltonian model describing an ac-driven electron in the one-dimensional multiple-well potential $V(x)$ shown in Fig. 1, it is well known that owing to the invariance of the potential $V(x)$ and of the dipole interaction term $xE(t)$ under simultaneous spatial reflection $x\to -x$ and time translation $t\to t+T/2$, the Floquet states ψ_l have a well-defined parity under such a variable transformation (dynamic or generalized parity; see, for instance, Ref. 6). In the corresponding NNTB model, which is expressed by Eqs. (2) and (4), it is thus expected that the Floquet states ψ_l should have a well-defined dynamic parity for simultaneous "discrete" reflection $n\to N-n+1$ and time translation $t\to t+T/2$. This can be explicitly demonstrated as follows. If $\psi_l(t)=u_n^{(l)}(t)$ is an eigenfunction of $\mathcal{H}$ with quasienergy E_l, after the time translation $t\to t+T/2$ from Eqs. (A1)–(A3), it is straightforward to show that $\psi_l'(t)\equiv u_{N-n+1}^{(l)}(t+T/2)$ is also an eigenfunction of $\mathcal{H}$ corresponding to the same quasienergy E_l. Therefore, both $\psi_l^{\pm}=1/\sqrt{2}(\psi_l\pm\psi_l')$ are eigenfunctions of $\mathcal{H}$ corresponding to the same quasienergy. If the eigenvalue E_l is not degenerate,

one thus must have $\psi_l^+=0$, i.e., $\psi_l'=-\psi_l$ or $\psi_l^-=0$, i.e., $\psi_l'=\psi_l$. This means that the periodic part $\psi_l=u_n^{(l)}(t)$ of Floquet states has a well-defined generalized parity according to Eqs. (51) and (52) given in the text. On the other hand, if the eigenvalue E_l is degenerate and ψ_l and ψ_l' are linearly independent, in place of them, one can choose $\psi_l^{\pm}$, which have again a well-defined and opposed parity.

The parity (even or odd) of a Floquet state ψ_l can be easily determined by adiabatically switching off the ac-driven field, i.e., by taking the limit $\mathcal{E}_0\to 0$. For $\mathcal{E}_0=0$, one has $F(t)=1$ and the eigenmodes q_l of Eq. (4) and corresponding energies e_l can be calculated in a closed form and read

$$q_l=\sqrt{\frac{2}{N+1}}\sin\left(\frac{\pi n l}{N+1}\right), \tag{A5}$$

$$e_l=2\Delta\cos\left(\frac{l\pi}{N+1}\right) \tag{A6}$$

$(l,n=1,2,3,\ldots,N)$. As the Floquet states $\psi_l(\mathcal{E}_0)$ and corresponding quasienergies $E_l(\mathcal{E}_0)$ are continuous functions of $\mathcal{E}_0$, a connection between $\psi_l(\mathcal{E}_0)$ and the eigenmode q_l given by Eq. (A5) [and, correspondingly, between quasienergy E_l and the energy e_l given by Eq. (A6)] should be established in the limit $\mathcal{E}_0\to 0$. To this aim, note that for a given mode index l, there will always exist an integer number m_l such that $e_l-m_l\hbar\omega$ falls inside the first Brillouin zone, i.e., $-\hbar\omega/2\le e_l-m_l\hbar\omega<\hbar\omega/2$. The integer m_l basically counts how many photons have to be subtracted from the undriven energy level e_l in order to arrive at the first Brillouin zone. The connection is thus simply established by Eq. (54) given in the text. As a particular case, assume that for any mode index l, one has $m_l=0$, a situation which surely occurs when the modulation frequency ω is larger than 4Δ [see Eq. (A6)]. In this case, from Eq. (A5), it follows that at $\mathcal{E}_0=0$, the Floquet state ψ_l with l even has an odd parity for the discrete reflection $n\to N-n+1$, whereas the Floquet state ψ_l with l odd has an even parity for discrete reflection. The same generalized parity is maintained as $\mathcal{E}_0$ is adiabatically switched on.

Finally, from Eqs. (A1)–(A3) and using the property $F(t+T/2)=F^*(t)$, Eq. (53) given in the text can be readily proved.

APPENDIX B: QUASIENERGY CROSSINGS AND AVOIDED CROSSINGS NEAR A COLLAPSE POINT

In this appendix, we present general results on crossings and avoided crossings of N quasienergies near a collapse point that can be deduced from the dynamical symmetries of the Floquet states. For the sake of definiteness, we will consider a sinusoidal electric field $E(t)=\mathcal{E}_0\cos(\omega t)$, however, the present analysis is valid for any ac field $E(t)$ such that $E(t+T/2)=-E(t)$. Let us assume a modulation frequency ω much larger than the hopping rate Δ and let us chose an electric field amplitude $\mathcal{E}_0$ close to the first collapse point of quasienergies, i.e., for which $\Gamma=ed\mathcal{E}_0/\hbar\omega$ is close to 2.405. Let us indicate by ψ_l and E_l the periodic parts of the Floquet states and corresponding nearly degenerate quasienergies for such a chosen electric field amplitude, and let us determine how the quasienergies are changed when the electric field amplitude is varied by a small amount $\delta\mathcal{E}_0$. Following Ref. 31, the quasienergies E and periodic parts ψ of the Floquet states for the varied electric field amplitude can be formally calculated from the perturbed eigenvalue equation

$$(\mathcal{H}_0+\delta\mathcal{H})\psi=E\psi, \tag{B1}$$

where $\mathcal{H}_0$ is given by Eqs. (A2) and (A3) for a field amplitude $\mathcal{E}_0$, whereas $\delta\mathcal{H}$ is the first-order correction term to $\mathcal{H}_0$ due to the small change $\delta\mathcal{E}_0$ in field amplitude. The explicit form of $\delta\mathcal{H}$ reads

$$\delta\mathcal{H}_{n,m}=\hbar\Delta\,\delta F(t)\,\delta_{n,m-1}+\hbar\Delta\,\delta F^*(t)\,\delta_{n,m+1}-i\hbar\frac{\partial}{\partial t}, \tag{B2}$$

where we have set

$$\delta F(t)=-i\frac{ed\,\delta\mathcal{E}_0}{\hbar\omega}\sin(\omega t)F_0(t) \tag{B3}$$

and $F_0(t)=\exp[-i(ed\mathcal{E}_0/\hbar\omega)\sin(\omega t)]$. Note that $\delta F(t+T/2)=\delta F^*(t)$. To determine the quasienergies E at the driving field amplitude $\mathcal{E}_0+\delta\mathcal{E}_0$, we can solve Eq. (B1) by a standard stationary perturbation theory for degenerate levels (see, for instance, Ref. 31). In fact, near the collapse point and in the large-frequency regime, all quasienergies E_l are nearly degenerate, as shown in Sec. III. We then search for a solution to Eq. (B1) of the form

$$\psi=\sum_{n=1}^{N}b_n\psi_n. \tag{B4}$$

Taking into account that $\mathcal{H}_0\psi_n=E_n\psi_n$, after substitution of Eq. (B4) into Eq. (B1) and taking the scalar product of both sides with ψ_l, we get the following homogeneous equations for the expansion amplitudes b_n:

$$(E-E_l)b_l=\sum_{n=1}^{N}V_{l,n}b_n, \tag{B5}$$

where we have set

$$V_{l,n}=\langle\psi_l|\delta\mathcal{H}|\psi_n\rangle=\sum_{m,r}\int_0^T dt u_m^{(l)*}(t)\,\delta\mathcal{H}_{m,r}u_r^{(n)}(t). \tag{B6}$$

Note that the coupling terms $V_{l,n}$ are proportional to $\delta\mathcal{E}_0$, i.e., one can write $V_{l,n}=v_{l,n}\delta\mathcal{E}_0$, with $v_{l,n}$ independent of $\delta\mathcal{E}_0$. In order to solve Eq. (B5), the following determinantal equation must be satisfied

$$\begin{vmatrix} E-\epsilon_1 & -V_{1,2} & -V_{1,3} & \ldots & -V_{1,N} \\ -V_{2,1} & E-\epsilon_2 & -V_{2,3} & \ldots & -V_{2,N} \\ \ldots & \ldots & \ldots & \ldots & \ldots \\ -V_{N,1} & -V_{N,2} & -V_{N,3} & \ldots & E-\epsilon_N \end{vmatrix}=0, \tag{B7}$$

where we have set $\epsilon_n\equiv E_n+V_{n,n}$ $(n=1,2,\ldots,N)$. Equation (B7) determines the values of the N quasienergies E when the electric field amplitude is varied by $\delta\mathcal{E}_0$ from the unperturbed value $\mathcal{E}_0$. As $\delta\mathcal{E}_0$ is continuously varied, the N roots of Eq. (B7) describe N curves which may show crossings

and/or avoided crossings depending on the generalized symmetries of the Floquet states and on the number N of levels. For instance, in the simplest case of two levels ($N=2$), Eq. (B7) yields

$$E = \frac{\epsilon_1 + \epsilon_2}{2} \pm \sqrt{\left(\frac{\epsilon_1 - \epsilon_2}{2}\right)^2 + |V_{1,2}|^2}. \tag{B8}$$

To obtain exact level crossing, one should simultaneously has $\epsilon_1=\epsilon_2$ and $V_{1,2}=0$. This condition is, in general, not possible to be satisfied by varying only one parameter (e.g., $\delta\mathcal{E}_0$), unless $V_{1,2}$ identically vanishes owing to symmetry reasons. Such a case occurs whenever the two Floquet states ψ_1 and ψ_2 have opposite generalized parity. Therefore, for the interaction of two nearly degenerate quasienergies, one obtains the well-known result that an exact level crossing is possible for two quasienergies belonging to the Floquet states with opposite dynamic parity, whereas an avoided crossing is observed in the opposite case (see, for instance, Refs. 6 and 31). For the interaction of more than two nearly degenerate quasienergies, a complex combination of crossings and avoided crossings is, in general, obtained. For our specific model defined by Eqs. (B1)–(B3), it can be easily shown that owing to the generalized symmetries of the Floquet states ψ_l summarized in Sec. IV A and derived in Appendix A, the following properties hold:

(i) $V_{l,n}=0$ whenever the Floquet states ψ_l and ψ_n have opposite generalized parity.
(ii) $V_{l,n}=0$ for $n=N+1-l$.
(iii) $V_{l,l}=-V_{n,n}$ for $n=N+1-l$, and therefore $\epsilon_{N+1-l}=-\epsilon_l$.
(iv) $V_{N-l+1,N-n+1}=-V_{n,l}$.

Such properties largely simply the problem of determining the pattern of level crossings and/or anticrossings near the collapse point for a multiple-well system. We discuss here in detail the cases corresponding to $N=3$ and $N=4$ wells, although the analysis can be extended to chains with a larger number of wells.

For a triple-well system ($N=3$), ψ_1 and ψ_3 have an even parity, whereas ψ_2 has an odd parity. Therefore, $V_{1,2}=V_{2,3}=0$. Moreover, for the properties (ii) and (iii) stated above, one also has $V_{1,3}=\epsilon_2=0$ and $\epsilon_3=-\epsilon_1$. Determinantal (B7) then reads

$$\begin{vmatrix} E-\epsilon_1 & 0 & 0 \\ 0 & E & 0 \\ 0 & 0 & E+\epsilon_1 \end{vmatrix} = 0, \tag{B9}$$

which yields the three roots

$$E=\epsilon_1,\ E=0,\ E=-\epsilon_1, \tag{B10}$$

with $\epsilon_1=E_1+v_{1,1}\delta\mathcal{E}_0$. Therefore, as $\delta\mathcal{E}_0$ is varied an exact level crossing for the three quasienergies is attained at $\delta\mathcal{E}_0=-E_1/v_{1,1}$, as shown in the insets of Fig. 3.

For a chain made of $N=4$ wells, ψ_1 and ψ_3 are even states, whereas ψ_2 and ψ_4 are odd states. Using the properties (i)–(iv) listed above, one then readily obtains $V_{1,2}=V_{1,4}=V_{2,3}=V_{3,4}=0$, $\epsilon_3=-\epsilon_2$, $\epsilon_4=-\epsilon_1$, and $V_{1,3}=-V_{2,4}$. Determinantal (B7) then yields the quadratic equation in E^2,

$$E^4 - E^2(\epsilon_1^2 + \epsilon_2^2 + 2|V_{1,3}|^2) + (\epsilon_1\epsilon_2 + |V_{1,3}|^2)^2 = 0, \tag{B11}$$

with $\epsilon_1=E_1+V_{1,1}$ and $\epsilon_2=E_2+V_{2,2}$. The behavior of the four quasienergy curves as functions of Γ depicted in Fig. 4(a) is compatible with Eq. (B11). In fact, an inspection of Eq. (B11) shows that possible level crossings may be observed at either $\epsilon_1=\epsilon_2$ or $\epsilon_1\epsilon_2+|V_{1,3}|^2=0$.

In the former case ($\epsilon_1=\epsilon_2$), which corresponds to $\Gamma=\Gamma_2$ in Fig. 4(a), Eq. (B11) has two distinct roots $E=\pm(\epsilon_1^2+|V_{1,3}|^2)^{1/2}$, each of them being twice degenerate, so that a pair of crossings between two quasienergy branches is attained. Note that the condition $\epsilon_1=\epsilon_2$ is satisfied for a single value of $\delta\mathcal{E}_0$, namely, $\delta\mathcal{E}_0=(E_2-E_1)/(v_{1,1}-v_{2,2})$.

The latter case ($\epsilon_1\epsilon_2+|V_{1,3}|^2=0$), which would correspond to $E=0$ being a doubly degenerate root of Eq. (B11), is found for a field variation $\delta\mathcal{E}_0$ satisfying the algebraic equation

$$(v_{1,1}v_{2,2} + |v_{1,3}|^2)\delta\mathcal{E}_0^2 + (E_2v_{1,1} + E_1v_{2,2})\delta\mathcal{E}_0 + E_1E_2 = 0. \tag{B12}$$

Equation (B12) may admit (i) two, (ii) one, or (iii) zero real-valued roots depending on the values of coefficients E_1, E_2, $v_{1,1}$, $v_{2,2}$, and $v_{1,3}$. The first case (i) does not seem to be applicable to our specific model, and therefore we just briefly discuss the other two cases. Case (ii) corresponds to point $\Gamma=\Gamma_1$ of Fig. 4(a) and is attained if $v_{1,1}v_{2,2}\simeq-|v_{1,3}|^2$. As shown in Fig. 4(a), two specular quasienergy branches are locally parabolic and touch each other at the vertex, without, however, effectively crossing.[32] Case (iii) corresponds, on the other hand, to an effective avoided crossing, in which the two specular and locally parabolic energy branches do not touch in the vertex (see, for instance, the inset of Fig. 4(a) in Ref.18). We can thus refer the level interaction at $\Gamma=\Gamma_1$ in Fig. 4 as an avoided crossing.

[1] M. Glück, A. R. Kolovsky, and H. J. Korsch, Phys. Rep. **366**, 103 (2002).
[2] S. Kohler, J. Lehmann, and P. Hänggi, Phys. Rep. **406**, 379 (2005).
[3] M. Holthaus and D. W. Hone, Philos. Mag. B **74**, 105 (1996).
[4] M. Grifoni and P. Hänggi, Phys. Rep. **304**, 229 (1998).
[5] V. M. Kenkre and S. Raghavan, J. Opt. B: Quantum Semiclassical Opt. **2**, 686 (2000).
[6] F. Großmann, T. Dittrich, P. Jung, and P. Hänggi, Phys. Rev. Lett. **67**, 516 (1991); F. Grossmann, P. Jung, T. Dittrich, and P. Hänggi, Z. Phys. B: Condens. Matter **84**, 315 (1991).
[7] D. H. Dunlap and V. M. Kenkre, Phys. Rev. B **34**, 3625 (1986).
[8] M. Holthaus, Phys. Rev. Lett. **69**, 351 (1992); M. Holthaus and D. Hone, Phys. Rev. B **47**, 6499 (1993).

[9] A. Zhang, L. Yang, and M. M. Dignam, Phys. Rev. B **67**, 205318 (2003).
[10] J. R. Madureira, P. A. Schulz, and M. Z. Maialle, Phys. Rev. B **70**, 033309 (2004).
[11] B. J. Keay, S. Zeuner, S. J. Allen, K. D. Maranowski, A. C. Gossard, U. Bhattacharya, and M. J. W. Rodwell, Phys. Rev. Lett. **75**, 4102 (1995).
[12] F. Großmann and P. Hänggi, Europhys. Lett. **18**, 571 (1992).
[13] J. M. Gomez Llorente and J. Plata, Phys. Rev. A **45**, R6958 (1992); J. M. Llorente and J. Plata, Phys. Rev. E **49**, 3547 (1994).
[14] Y. Kayanuma, Phys. Rev. A **50**, 843 (1994).
[15] J. C. A. Barata and W. F. Wreszinski, Phys. Rev. Lett. **84**, 2112 (2000); J. C. A. Barata and D. A. Cortez, J. Math. Phys. **44**, 1937 (2003).
[16] C. E. Creffield, Phys. Rev. B **67**, 165301 (2003).
[17] J. Karczmarek, M. Stott, and M. Ivanov, Phys. Rev. A **60**, R4225 (1999).
[18] J.M. Villas-Bôas, S.E. Ulloa, and N. Studart, Phys. Rev. B **70**, 041302(R) (2004).
[19] K. Saito and Y. Kayanuma, Phys. Rev. B **70**, 201304(R) (2004).
[20] P. Marquetand, S. Gräfe, D. Scheidel, and V. Engel, J. Chem. Phys. **124**, 054325 (2006).
[21] S. Raghavan, V. M. Kenkre, D. H. Dunlap, A. R. Bishop, and M. I. Salkola, Phys. Rev. A **54**, R1781 (1996).
[22] M. Frasca, Phys. Rev. B **71**, 073301 (2005).
[23] P. H. Rivera and P. A. Schulz, Phys. Rev. B **61**, R7865 (2000).
[24] A.-Z. Zhang, P. Zhang, D. Suqing, X.-G. Zhao, and J.-Q. Liang, Phys. Rev. B **63**, 045319 (2001).
[25] For optimal CDT at low modulation frequencies, a better choice for the phase φ would be $\varphi=\pi/2$ (see, for instance, Ref. 18). However, the phase φ does not change the long-time behavior of tunneling dynamics, which is of main interest in the present analysis.
[26] A. Peres, Phys. Rev. Lett. **67**, 158 (1991).
[27] M. Latka, P. Grigolini, and B. J. West, Phys. Rev. A **50**, 1071 (1994).
[28] J. Y. Shin and H. W. Lee, Phys. Rev. E **53**, 3096 (1996).
[29] P. Zhang and X.-G. Zhao, Phys. Lett. A **271**, 419 (2000).
[30] J. von Neumann and E. P. Wigner, Z. Phys. **30**, 467 (1929).
[31] L. D. Landau and E. M. Lifshitz, *Quantum Mechanics*, 3rd ed. (Pergamon, Oxford, 1977), Sec. 79.
[32] This is the case found in framework of the third-order perturbative theory [see, Eq. (65)], which is in agreement with numerical simulations at small values of Δ/ω. As Δ/ω increases, Γ_1 is resolved as an avoided level crossing.